Jpn. J. Appl. Phys. Vol. 42 (2003) pp. 7354–7360
Part 1, No. 12, December 2003

Capacitively Coupled Discharges as Photoionization Sources in an Electrode-Dielectric-Screen Assembly

Jorge NIEDBALSKI

Consejo Nacional de Investigaciones Científicas y Técnicas (CONICET), Centro de Investigaciones en Láseres y Aplicaciones CEILAP (CITEFA-CONICET), Juan Bautista de La Salle 4397, (B1603ALO) - Villa Martelli, Buenos Aires, Argentina

(Received January 6, 2003; accepted June 23, 2003; published December 10, 2003)

The influence of the dielectric material and the dependence of parameters (pressure, voltage, etc.) on the development of volumetric gas discharges as photoionization sources in a capacitively coupled (electrode-dielectric-screen) assembly were investigated. Two materials with very different permittivity values and high contrast in their hysteresis effects were tested in assemblies excited by high-voltage pulses with a rise time of about 5 ns within the range 5–11 kV. Discharges in nitrogen and neon gases were characterized in detail through the measurements of current and emitted light to establish the necessary conditions for an optimized performance (uniformity and intensity) of irradiation. A comparison between the two assemblies as to the production of phototriggered discharges within regions behind a single and a double screen subjected to a uniform electric field was performed. [DOI: 10.1143/JJAP.42.7354]

KEYWORDS: high-voltage discharge, dielectric, permittivity, hysteresis, screen, photoionization, plasma, glow discharge, gaseous laser

1. Introduction

Capacitively coupled discharges (CCDs), sometimes referred to as corona discharges, are currently used as ultraviolet (UV) preionization sources in a number of transversely excited lasers including nitrogen, carbon dioxide and excimer lasers. Among the various assemblies in which this technique could be adopted to irradiate relatively large volumes of gas,[1–10] one which supplies radiation from behind a cathode screen[5–10] probably constitutes the most effective due to its optimal geometrical adaptation (by its very close proximity) to the laser channel, which allows it to generate both sufficient density and a uniform distribution of photoelectrons in the neighborhood of the cathode surface to stabilize self-sustained pumping discharges.

To our knowledge, very little detailed information on the general character of the discharges (nature and temporal behavior) produced in such an assembly to establish optimum operating conditions for irradiation is available in the literature. Until now, the most relevant work devoted to this issue was performed with CCDs subjected to a highly nonuniform and very intense electric field, which develop as streamers over the dielectric surface.[11]

Here, we are interested in determining the initial conditions and physical mechanism of volumetric gas discharge within the dielectric-screen region, as well as the influence presented to its subsequent development by the dielectric material properties, i.e., type of gas, screen and parameters. To this purpose, two materials with very different permittivity values and high contrast in their hysteresis effects were tested for discharges performed in typical gases used with lasers.

The main goal of this work is to gain insight on the performance of an electrode-dielectric-screen assembly as a photoionization source.

In §3 we give a rough estimate of the order of magnitude of the expected gas discharge current peak for each dielectric material, starting from a simplified theoretical model of charge accumulation at its surface. Current and light emission intensity measurements associated with homogeneous (glow) discharges in neon and nitrogen gases as a function of the parameters that can be modified in the assembly are presented in §4.1 and §4.2.

In §4.3 the assemblies are compared as to the production of phototriggered discharges within regions behind a single and a double screen subjected to a uniform electric field. A very simple test which reveals the presence of bremsstrahlung soft X-rays in the photoionizing radiation spectrum is also reported.

Finally, conclusions are drawn in §5.

2. Device

Figure 1 shows a cross-sectional view of the device constructed for this study. The discharge cell is of transparent Lucite and it consists of two independent sections united at the center. The capacitively coupled assembly (CCA) in the upper section featured a circular brass plate

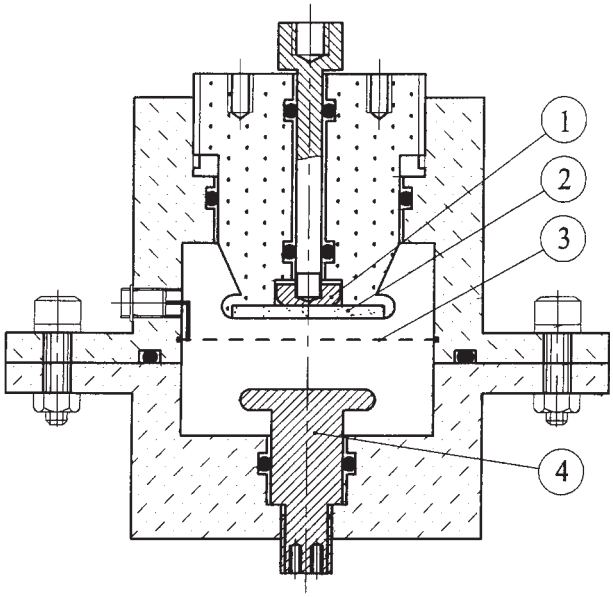

Fig. 1. Cross-sectional view of the experimental device. (1) High-voltage electrode (13 mm diameter), (2) dielectric plate (glass or ceramic), (3) stainless steel screen (60% transparent), (4) uniform field electrode (35 mm diameter).

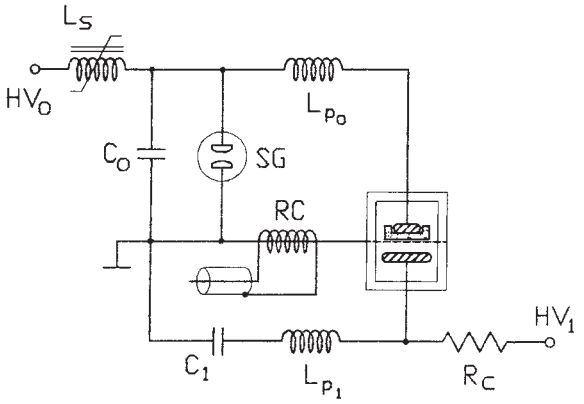

Fig. 2. Circuit diagram of the experimental setup. L_s: saturable inductor, C_o: 480 pF capacitor, C_1: 1000 pF capacitor, SG: coaxial spark gap, RC: Rogowski coil, R_c: 10-MΩ resistor, Lp_o and Lp_1: parasitic inductances.

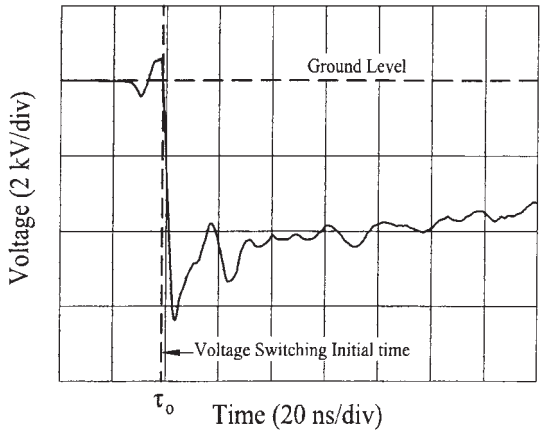

Fig. 3. Voltage waveform applied to the CCA.

(high-voltage electrode) of 13 mm diameter whose contour was shaped to minimize the electric field enhancement. This electrode was pressed against a dielectric plate fixed with epoxy adhesive to a holder which can be displaced from zero up to 5 mm with respect to a screen (connected to ground potential) of 60% transparency. The screen was chosen from among commercially available ones; it was manufactured by perforating a 0.4 mm thick stainless steel sheet. Small imperfections (burrs) present on one of the surfaces were removed.

Two dielectric materials with relative permittivity ε_{ri} were separately tested: borosilicate glass 1 mm thick with $\varepsilon_{rg} \approx 7$ and ceramic ($BaTiO_3$) 3 mm thick with $\varepsilon_{rc} \sim 4500$. Hereinafter, the subscripts g and c will be employed to represent the glass and ceramic, respectively. The ceramic plate was obtained by cutting a commercial capacitor. The material was identified by X-ray diffraction using a Phillips diffractometer (Model 3710). The permittivity was estimated from the geometrical dimensions of the assembly and its capacitance, which was measured at low voltage (3 V) and low frequency (~800 Hz) using a digital capacitometer. A uniform field electrode of 35 mm diameter was installed at the bottom of the cell to drive the main discharge when it was directly triggered by photoionization. The circuit diagram of the experimental setup is shown in Fig. 2. The CCAs were energized by the capacitor with $C_0 \approx 480$ pF, which was made of a double-sided copper fiberglass circuit board, and can be dc charged up to 13 kV and switched through a low-inductance, self-triggered coaxial spark gap (SG).[12] This arrangement provides a voltage inversion to the CCAs without oscillation and with a rise time of about 5 ns. Figure 3 shows a typical voltage waveform monitored using a capacitive probe[13,14] and displayed on a digital oscilloscope (HP 54510 A). A self-integrating Rogowski coil (RC), installed as shown in Fig. 2, was employed for monitoring both discharge currents.

3. Estimation of the Charge and Current Densities Associated with the Capacitively Coupled Discharges

A schematic cross section of the discharge region is shown in Fig. 4. The circular high-voltage electrode of area A is separated from the screen by a vacuum region, and touches a dielectric of thickness t and low-frequency relative

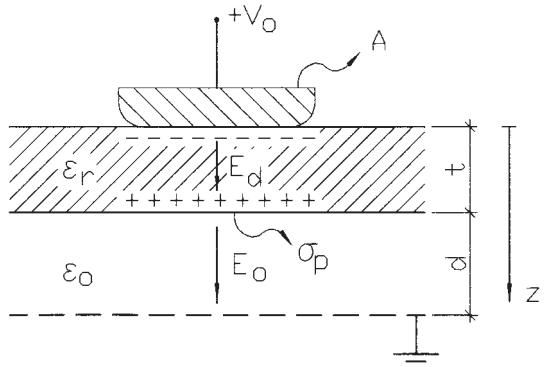

Fig. 4. Schematic cross section of the CCA. V_o: charging voltage, A: area of the high-voltage electrode, ε_r: relative dielectric permittivity, E_d: electric field within the dielectric region, t: thickness of the dielectric, σ_p: polarization charge density, ε_o: vacuum permittivity, E_o: electric field within the vacuum region, d: dielectric-screen gap separation.

permittivity ε_r. The assembly capacitance is given by

$$C_a = \varepsilon_r \varepsilon_o A/(\varepsilon_r d + t), \tag{1}$$

where ε_o is the vacuum permittivity and d the dielectric-screen gap separation. The slow application of a dc voltage V_o to the assembly produces polarization of the dielectric induced by the electric field across the interelectrode gap. The free charge density σ_f at the high-voltage electrode can be deduced either from eq. (1) or by applying the line integral of the electric field through both the dielectric ($E_d = \sigma_f/\varepsilon_r\varepsilon_o$) and vacuum ($E_o = \sigma_f/\varepsilon_o$) regions.

$$\int_0^{t+d} E\, dz = \sigma_f[(t/\varepsilon_r) + d]/\varepsilon_o = V_o \tag{2}$$

From eq. (2) we can obtain

$$\sigma_f = \varepsilon_o V_o/[(t/\varepsilon_r) + d]. \tag{3}$$

The relationship between the free charge density and the polarization charge density σ_p at the dielectric surface is given by

$$\sigma_p = (\varepsilon_r - 1)\sigma_f/\varepsilon_r. \tag{4}$$

Substituting σ_f of eq. (3) into eq. (4), we obtain

$$\sigma_p = \varepsilon_o(\varepsilon_r - 1)V_o/\varepsilon_r[(t/\varepsilon_r) + d]. \quad (5)$$

The well-known eq. (5) should be partially modified by making $d = 0$ when the dielectric-screen region is filled either with a gas at low pressure or with a gas of low dc dielectric strength. In fact, under such conditions, if the voltage is slowly raised to V_o, a transient flux of electrons transported through the gas from the ground screen to the dielectric should be established. As a consequence, a charge accumulation of surface density $\sigma_s \approx \sigma_p$ ($d = 0$) would arise on the dielectric surface (z dependence is neglected) to cause the quasi cancellation of the electric field within the gas-filled region. Experimental evidence of the occurrence of this process was obtained in the course of this work using neon gas in the device illustrated in Fig. 1: a) during the application of voltage V_o, light emission was always observed and b) voltage can be maintained even for values that greatly exceed the gas dc self-breakdown threshold voltage. This surface charge distribution must then be considered to specify the initial conditions for gas discharge. Note that for an efficient transport of charges via the gas, the possible pressure range (p) is basically conditioned by d, V_o and the dc dielectric strength (S) of the gas. Such a condition can be mathematically expressed by the relationship $E_o/S \gg 1$. On the contrary, when $E_o/S \ll 1$, the gas acts as an insulating medium. Thereafter, if a fast voltage inversion (of the order of V_o in time τ) is applied to the CCA, a change of the charge distribution on the dielectric surface would be expected. The magnitude of the charge involved (physically driven by the displacement current inside the dielectric medium) may roughly be determined by replacing the permittivity value at low frequency, ε_r, in eq. (5) by the corresponding $\varepsilon^*{}_r \equiv \varepsilon_r(f)$ for the frequency ($f = 1/\tau$) at which the electric field changes during the voltage inversion. Thus, the density of charge released from the dielectric surface is given by

$$\sigma^*{}_s \approx \varepsilon_o[\varepsilon^*{}_r - 1]V_o/t, \quad (6)$$

and the current density associated to the gas discharge is estimated as

$$J_c \approx \sigma^*{}_s/\tau. \quad (7)$$

In order to quantify $\sigma^*{}_s$ and J_c for typical discharge parameters ($\tau = 5\,\text{ns}$ and $V_o = 5.5\,\text{kV}$), the permittivity values of each dielectric material used in the CCA were compared within the range of 100–400 MHz employing an HP 4291A impedance-material analyzer. In contrast to the quasi-constant values of $\varepsilon^*{}_{rg} \approx 7$ found for borosilicate glass within that frequency range, the ceramic exhibited significant variations in addition to a pronounced hysteresis effect (*e.g.*, the polarization inside this material does not proportionally follow the external electric field changes). In particular, at the frequency $f = 1/5\,\text{ns} = 200\,\text{MHz}$, the value measured was $\varepsilon^*{}_{rc} \approx 320$. Using these data in eqs. (6) and (7) gives $\sigma^*{}_{sg} \approx 292\,\mu\text{C/m}^2$, $J_{cg} \approx 58\,\text{kA/m}^2$, $\sigma^*{}_{sc} = 5.2\,\text{mC/m}^2$ and $J_{cc} \approx 1.04\,\text{MA/m}^2$. For the area of the high-voltage electrode, $A = 1.3 \times 10^{-4}\,\text{m}^2$, the corresponding gas discharge current peaks ($I_{ci} = J_{ci}\,A$) will be $I_{cg} \approx 7.6\,\text{A}$ and $I_{cc} \approx 138\,\text{A}$.

In general, according to the simplified analysis described in this section, under the conditions where $E_o/S \gg 1$ and similar discharge parameters, the expected current peak values for the ceramic might be two orders of magnitude greater than that for the glass.

4. Experimental Results

Volumetric gas discharges within the dielectric-screen region were characterized by visual inspection and by current and emitted light intensity measurements as a function of parameters that may be varied in the CCA. The CCAs were driven at voltages V_o between 5 and 11 kV with a repetition rate of about 0.5 Hz. The employed gases were nitrogen and neon pressurized in the cell within the static range of 5–100 kPa; the two gases were chosen on the basis of their very different dc dielectric strengths and also because of their use as a laser medium (nitrogen) and buffer (neon) in rare-gas halide mixtures.

4.1 Discharge features

Once the initial charge (electrons) accumulation on the dielectric surface is achieved, as described in §3, discharge starts within the dielectric-screen region when the spark gap SG (see Fig. 2) is closed. During the time in which the voltage inversion occurs, the electrons released from the surface are transferred to the gas and accelerated across the gap, producing excitation and ionization mainly by direct collisions with other species (atoms or molecules). The dynamics of that process is assumed to be controlled predominantly by the hysteresis and permittivity of the dielectric material, which determinate the rate of current rise in the formed plasma and the time taken until the dielectric discharge, respectively. In what follows, this assumption will be experimentally confirmed.

In order to find the first clue to the nature of the gas discharge and how it varies when the parameters p and d are modified, the discharges were visually inspected in a dark environment from behind a screen through a transparent plate, installed after removing the bottom of the cell. The formation of uniform light spots in the screen plane, as produced by homogeneous (glow) discharges and roughly delineated by the high-voltage electrode area, were typically observed in neon throughout the entire pressure range (up to 100 kPa) for $d \approx 0.3\,\text{mm}$ and $d = 1\,\text{mm}$, and up to about 55 kPa for $d = 2\,\text{mm}$. In nitrogen, discharges with similar features were strongly restricted to pressures only up to about 35 kPa for $d \approx 0.3\,\text{mm}$, 10 kPa for $d = 1\,\text{mm}$ and 7–8 kPa for $d = 2\,\text{mm}$. Variations at higher p and/or larger d values were manifested as a gradual transition to filamentary channels superimposed on a weak diffuse background which appeared in the screen plane as a nonuniform distribution of very intense luminous points. The screen employed in the CCAs was also found to influence the nature of the discharges. For example, when the actual screen was replaced by another popularly known as the "mosquito net", the number of filamentary channels was significantly increased under similar discharge conditions.

Figures 5 and 6 are reproductions of typical current waveforms corresponding to discharges in neon, as recorded in separated tests, with glass and ceramic in the CCA for $V_o = 5.5\,\text{kV}$ and 9.2 kV, respectively, $d \approx 0.3\,\text{mm}$ and $p = 10\,\text{kPa}$. For the CCA with glass, after the initial peak associated with the proper dielectric discharge (indicated by

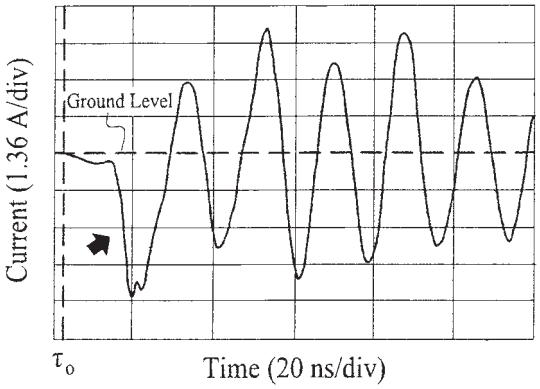

Fig. 5. Temporal evolution of the current associated with discharges in neon gas with glass in the CCA. The arrow indicates the current originating from the charge that initially was accumulated at the dielectric surface. Discharge parameters were $V_o = 5.5\,\text{kV}$, $p = 10\,\text{kPa}$ and $d \approx 0.3\,\text{mm}$.

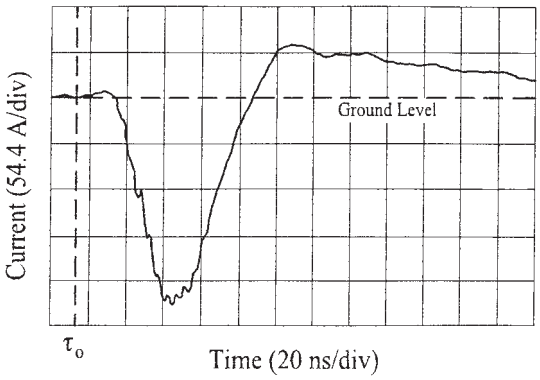

Fig. 6. Temporal evolution of the current associated with discharges in neon gas with ceramic in the CCA. Discharge parameters were $V_o = 9.2\,\text{kV}$, $p = 10\,\text{kPa}$ and $d \approx 0.3\,\text{mm}$.

the arrow in Fig. 5), the oscillatory behavior observed is a consequence of the high C_o/C_A ratio ($\approx$480/8) in the circuit of Fig. 2, where $C_A = 8\,\text{pF}$ is the assembly capacitance. Once the voltage variation reaches the maximum, the Lp_o–C_o–C_A–Z_g subcircuit (Z_g represents the gas impedance) is forced to oscillate due to the residual voltage at C_o during its relatively long decay time. This oscillation could easily be removed by operating the subcircuit under an overdamped condition, for instance, by connecting at its ground return a series load resistor.

The experimental current peak values (I^E_{ci}) in Figs. 5 and 6 ($I^E_{cg} \approx 5.4\,\text{A}$ and $I^E_{cc} \approx 234\,\text{A}$) are in reasonably good agreement with those theoretically estimated by the simple analysis described in §3. Furthermore, the above-mentioned assumption about the influence of hysteresis and permittivity of the dielectric materials on the response at the same applied voltage inversion, is confirmed by the very dissimilar temporal evolution of the two discharge currents.

Figure 7 illustrates the dependence of I^E_{ci} on d with glass and ceramic in the CCA for $V_o = 5.5\,\text{kV}$ and $p = 10\,\text{kPa}$. The solid and dashed lines represent the results for neon and nitrogen, respectively. A change of scale was used for the current axis to allow the comparison of the curves. Each data point is the average of 16 values corresponding to consec-

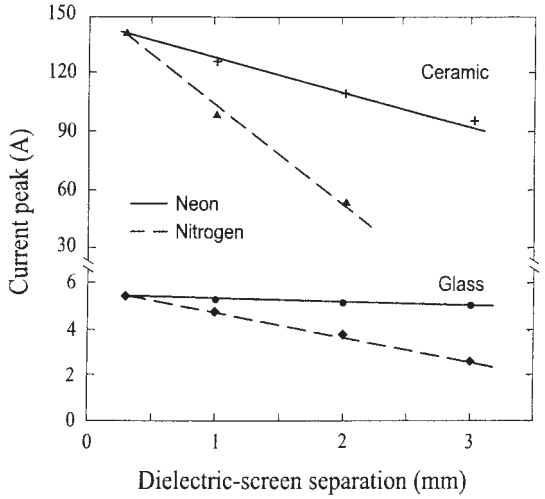

Fig. 7. Variation of the current peak corresponding to discharges in neon and nitrogen gases as a function of the dielectric-screen gap separation (d) with ceramic (upper) and glass (lower) in the CCA, for $V_o = 5.5\,\text{kV}$ and $p = 10\,\text{kPa}$. A change of scale was used in the current axis to allow the comparison of the four curves.

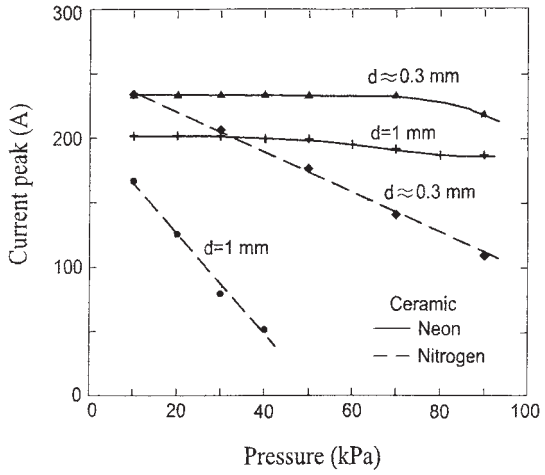

Fig. 8. Variation of the current peak corresponding to discharges in neon and nitrogen, with ceramic in the CCA, as a function of pressure for two dielectric-screen gap separations (d) and $V_o = 9.2\,\text{kV}$.

utive pulses on each of four series of shots. Typically, I^E_{ci} varied up to $\pm 10\%$ among repeated shots. In Fig. 8, I^E_{ci} is plotted against p with ceramic in the CCA for $V_o = 9.2\,\text{kV}$, $d \approx 0.3\,\text{mm}$ and $d = 1\,\text{mm}$. It is clear from the figures the I^E_{ci} (basically dependent on the initial process of charge accumulation at the dielectric surface) is affected by the dielectric strength of each gas and by both p and d parameters. Other measurements, which are not presented here because of the space limitation, indicate that I^E_{ci} linearly increases as V_o is increased.

The temporal evolution of the current in helium discharges presented a behavior similar to that obtained with neon, although the current peak values were slightly lower.

4.2 Light emission

Light emitted by discharges was recorded at a distance of 6 cm from behind the screen using a fast photomultiplier (200 ps rise time) which had a cesium-antimony photo-

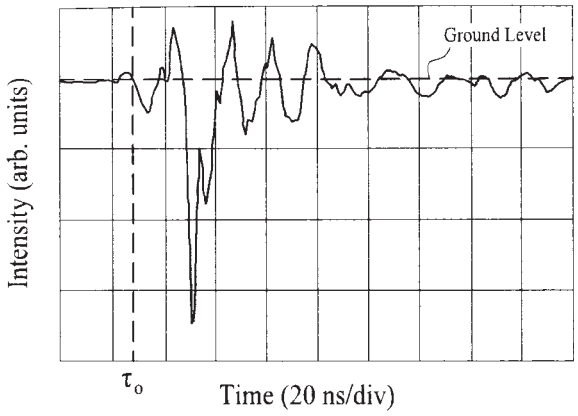

Fig. 9. Typical shape of the optical pulse emitted by discharges in neon, with glass in the CCA. The radiation was monitored at a distance of 6 cm from behind the screen using a fast photomultiplier. Discharge parameters were $V_o = 6.5\,\text{kV}$, $p = 10\,\text{kPa}$ and $d \approx 0.3\,\text{mm}$.

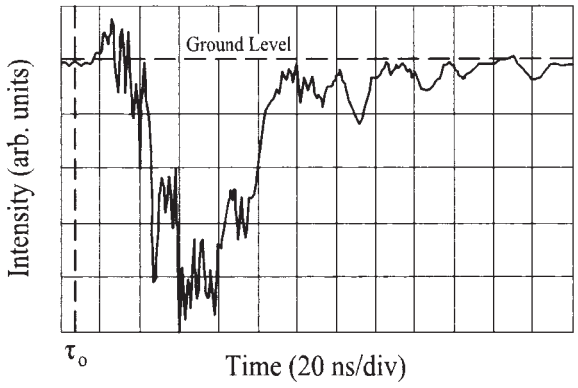

Fig. 10. Typical shape of the optical pulse emitted by discharges in neon, with ceramic in the CCA, obtained under the same conditions as described in Fig. 9.

cathode with spectral sensitivity extended from 210 to 640 nm, and the above-mentioned digital oscilloscope. The radiation flux was previously limited by the aperture of 10 mm diameter in an opaque Lucite plate where a BK7 optical window (nominal cutoff at 290 nm) was mounted; the plate and the optical window functioned to the pressure seal after removing the bottom of the discharge cell. A wavelength ranging from near-UV to red regions was selected through an optical filter, which served to prevent saturation of the photocathode. The temporal resolution of the detection system was about 2 ns. Figures 9 and 10 show optical pulses generated by discharges in neon with glass and ceramic in the CCA, respectively, for $V_o = 6.5\,\text{kV}$, $p = 10\,\text{kPa}$ and $d \approx 0.3\,\text{mm}$. These temporal behaviors were typical throughout the measurements. Note that for the CCA with glass, emission takes place only during the first half-cycle of the current pulse (Fig. 5) and the later oscillation contribute little to the selected wavelength band. For the CCA with ceramic, the series of spikes that appear in the signal was a result of the emission from the two gases and it was more intense in nitrogen. We speculate that those spikes are a consequence of the emission from faint current filaments (not directly visible) through low-impedance channels within the homogeneous discharge volume, and

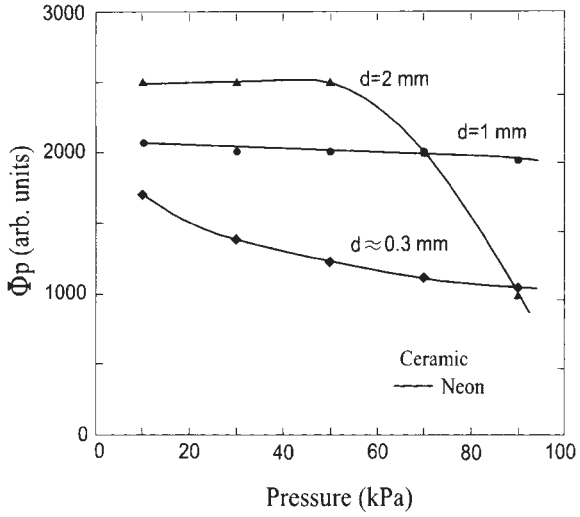

Fig. 11. Variation of the peak value (Φ_p) of the optical pulses emitted by discharges in neon as a function of pressure, with ceramic in the CCA, for three dielectric-screen gap separations (d) with $V_o = 6.5\,\text{kV}$.

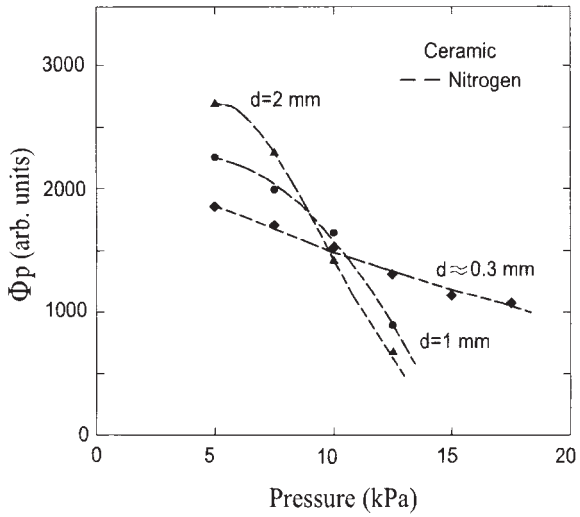

Fig. 12. Variation of the peak value (Φ_p) of the optical pulses emitted by discharges in nitrogen as a function of pressure, with ceramic in the CCA, for three dielectric-screen gap separations (d) with $V_o = 6.5\,\text{kV}$.

whose origin may be directly entailed to the dielectric material by any or both of the following two causes: inhomogeneities in its structure, particularly associated with a small "ferroelectric dominion", and injection of material in the gas in the form of vapor jets generated by the explosion of microirregularities present in the surface. The possibility of this last cause seemed to be confirmed by the fact that a fine powder of dielectric material is always found to be deposited on the screen after numerous shots, being particularly abundant when nitrogen is used.

The graphs in Figs. 11 and 12 show the variation of the peak value (Φ_p) of the optical pulses as a function of p. The pulses were emitted by discharges in neon and nitrogen, respectively, with ceramic in the CCA for $V_o = 6.5\,\text{kV}$ and taking d as a constant parameter. The measurements were performed by limiting the effective dc BW of the oscilloscope to about 30 MHz to remove the above-mentioned high-frequency components. Each data point represents the

average of 16 consecutive values. Clearly, Φ_p increases at a constant pressure as d is increased, which is consistent with the augmentation of the number of species excited within the major discharge volume. Also, the trend outlined by direct observation in the preceding section is quantitatively well supported in the case of neon (see Fig. 11), by the fall-off of intensity corresponding to the point ($d = 2$ mm, $p \approx 55$ kPa) where the discharge changed in nature; when this change occurs, a great deal of shot-to-shot variation in the optical signal is observed. Thus, these measurements give approximate ranges of p and d values in neon and nitrogen, within which adequate operating conditions for irradiation (uniformity and intensity) can be obtained. In particular, at pressures higher than about 55 kPa in neon, the best performance is obtained with $d \approx 1$ mm. The emission intensity was also found to increase proportionally with V_o, according to the higher current density and drift velocity of electrons in the discharges.

It should be noted that the photon energies within the selected wavelength region are far below that required to produce effective photoionization, via absorption of a single photon, in the same gas when the CCA is used as a source, namely $W_i = 14.5$ eV for nitrogen and 21.56 eV for neon (W_i is the ionization energy). Considering the wide variety of interactive processes tied at a gaseous discharge,[15] our interest for the present application is only on the hard emission, *e.g.*, $h\nu \geq W_i$ (h is Planck's constant and ν is the radiation frequency), which involves ionization as a result of the collisions of electrons with other species and typically represents a small fraction of the overall emission contribution given by the integral of the product of $F(W)$ (function distribution of electron energies in the discharge) with $\sigma_i(W)$ (function ionization cross section). Therefore, modifications in both temporal evolution and intensity of the optical pulses might be expected for those higher photon energies with respect to the obtained by gas excitation (Figs. 9 and 10).

4.3 Phototriggered discharge tests

The performance characteristic of the CCAs as preionization sources was compared as to the production of stable phototriggered discharges within the region behind the screen (main region) subjected to a uniform electric field. For these experiments neon was used as the test gas. To ensure good uniformity of irradiation within the entire pressure range, the dielectric-screen gap separation was set at 1 mm in accordance with data in Fig. 11, whereas to provide sufficient UV radiation intensity, V_o was varied from 8 to 11 kV. Energy for the main discharge was supplied by the capacitor $C_1 \approx 1000$ pF (see Fig. 2). Normally, most of this energy is dissipated into the gas volume which results in further extension with respect to that delineated by the area (A) of the high-voltage electrode of the CCA and the separation between the screen and the uniform field electrode ($D = 17$ mm). The sequential procedure for the experiment was as follows: first, the capacitor C_1 is dc charged to voltage V_1 (typically from 0.1 to 1.5 kV) which is close to the self-breakdown threshold V_{sb} corresponding to the gas for a given pressure; afterwards the CCA is excited by applying voltage V_o, and finally, the main region is irradiated when the spark gap SG is switched.

Operating the CCAs under similar conditions, the dissimilar photoelectron density levels were manifested near the screen surface by means of the voltage V_1 necessary to initiate and to support the uniform electron avalanche through gas. The critical difference found when stable glow discharges were obtained, was that the CCA with glass required, in every instance, a voltage V_1 very close to V_{sb} ($V_1/V_{sb} \approx 0.98$), whereas with ceramic, V_1 was 10–15% lower ($V_1/V_{sb} = 0.90$–0.85). A detrimental effect observed as a result of the shot-to-shot performance very close to V_{sb}, was the high probability of gas breakdown within the main region prior to the phototriggering signal, which caused the sequential procedure to become random. This could be attributable to transient fluctuations of the screen potential (nominally grounded) and/or the spurious UV radiation emitted from the weakly ionized gas within the dielectric-screen region, during the initial stage of charge transport towards the dielectric surface.

In general, the phototriggering phenomenon is directly observed as an overlap of the two discharges through the screen; whether homogeneous or filamentary discharges are designed to occur in the dielectric-screen region, for instance, by varying the parameters d and/or p, respectively, the same features are extended to the main region.

In order to assess the influence of the different temporal evolutions of the optical pulses on the main discharge, a second (identical) screen separated by 4 mm from the first, was incorporated in the device illustrated in Fig. 1. This provided reliability of the sequential procedure by preventing the irregular behavior above described. Here, the irradiated area was limited by a metallic plate having an orifice of 7 mm diameter, which was mounted on the second screen. Current pulses associated with stable discharges obtained under similar parametric conditions, except V_1 which was slightly higher in the case of the CCA with glass, did not show any appreciable differences. Figure 13 shows a typical current waveform for $V_o = 9.2$ kV, $p = 60$ kPa, $d = 1$ mm, $V_1 \approx 0.5$ kV and $D = 13$ mm.

Finally, the phototriggering method was used to investigate short-wavelength radiation components emitted from the CCAs. As has been demonstrated by Kremnev and Kurbatov.,[16] deceleration of electrons by collisions with other species in gas discharges subjected to relatively strong electric fields ($E_o/p \sim 0.037$–0.496 V/mm·Pa) is accompa-

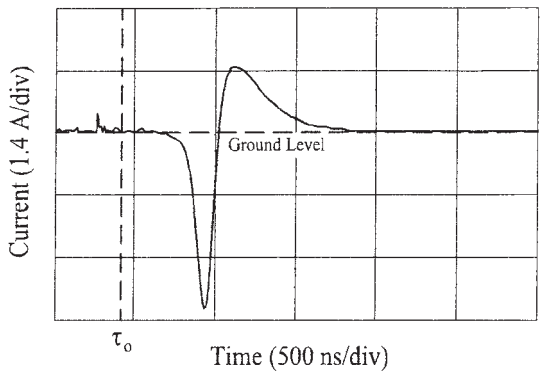

Fig. 13. Typical temporal evolution of the current pulse associated with stable phototriggered discharges in neon, obtained arbitrarily using glass or ceramic and a double screen in the CCA. Discharge parameters were $V_o = 9.2$ kV, $p = 60$ kPa, $d = 1$ mm, $V_1 \approx 0.5$ kV and $D = 13$ mm.

nied by the emission of X-rays. According to ref. 17, the overall photon energy irradiated via the bremsstrahlung would depend approximately linearly on the current density and the atomic number of the targets (species). Due to the high E_o/p ratios typically applied to the present CCAs, comparable to those reported in ref. 16, and to the relatively high current densities associated with discharges, particularly with the ceramic, a significant flux of X-rays might be expected. To investigate this, a CaF_2 filter (nominal cutoff at 123 nm) was inserted between screens. Under the above-described operation with $V_o = 9$–11 kV, stable discharges triggered by X-rays were observed to be formed up to about 100 kPa. No attempt was made to determine the highest energy of the photons of the resultant continuous spectrum. However, as a reference, when the optical filter was replaced by thin aluminum foil (5.4 mg/cm^2), the X-rays were either completely absorbed or the fraction transmitted was insufficient to induce even gas breakdown.

5. Conclusions

We carried out an experimental study on the production of volumetric gas discharges in an electrode-dielectric-screen assembly, which we believe, helps to elucidate the roles played by the dielectric material properties, the type of gas, the screen and the parameters. Thus it contributes to a better understanding of the performance of the assembly as a photoionization source. The main results can be summarized as follows.

(1) The direct observation during the slow application of the voltage V_o to the CCA, together with the small discrepancy found in the discharge current peaks for each dielectric material between those derived using the simple model described in §3 and those experimentally measured (§4.1), confirm that the necessary condition for the occurrence of discharges within the dielectric-screen region, is the prior accumulation of charges via gas at the dielectric surface. The major limiting factor of such an accumulation is the dielectric strength of the gas, which essentially controls the possible operating pressure range.

(2) In response to the high-voltage excitation pulse applied to the CCA, the dynamics of the gas discharge is mainly driven by the hysteresis and permittivity of the dielectric material which also determine the temporal behavior (rise rate and width) of the optical pulse emitted.

(3) The intensity and uniformity of irradiation can be optimized in a given gas through the control of the nature of the discharge within the dielectric-screen region by suitable selection of V_o and operating points (p and d). For neon, which exhibits a strong tendency to form glow discharges, in addition to a very low dielectric strength, the best performance is obtained for $d \approx 1$ mm throughout the entire pressure range (Fig. 11). In contrast, for nitrogen, the pressure range is limited up to about 10 kPa (Fig. 12).

(4) The choice of the type of screen is important for the present application.

(5) Phototriggering tests described in §4.3 reveled that a) when a single screen is used in the CCA, the degree of homogeneity of the discharge within the dielectric-screen region inexorably influence (by means of overlapping) the degree of homogeneity of that developed in the main region. In general, a double screen separated by a small gap can be used to break the physical continuity between the two discharges; b) using a dielectric material with high permittivity in the CCA, ensures, through discharges with high current densities, a concomitant radiation flux at lower wavelengths (soft X-rays) in addition to significant UV radiation flux. Therefore, practical operating conditions on the basis of a shot-to-shot performance can be achieved, due to the possibility of driving the main discharges at voltages V_1 well below V_{sb}; c) with conditions under which sufficient photoelectron density to initiate and to stabilize the main discharge is generated by irradiation, the temporal behavior of the current associated with this discharge is basically defined by the parameters (C_1 and Lp_1) of its driving circuit, making it independent of the temporal evolution of the preionizing optical pulse.

1) V. Hasson and H. V. von Bergmann: Rev. Sci. Instrum. **50** (1979) 1542.
2) F. Encinas Sanz and J. M. Guerra Perez: IEEE J. Quantum Electron. **27** (1991) 891.
3) A. Armandillo, G. Grasso and G. Salvetti: Rev. Sci. Instrum. **56** (1985) 674.
4) R. Gratton, S. Mangioni and J. Niedbalski: J. Phys. D **24** (1991) 11.
5) T. S. Fahlen: IEEE J. Quantum Electron. **15** (1979) 311.
6) R. C. Sze: J. Appl. Phys. **54** (1983) 1224.
7) R. S. Taylor and K. E. Leopold: J. Appl. Phys. **65** (1989) 22.
8) S. V. Effimovskii, A. K. Zhigalkin, Yu. I. Karev and S. V. Kurbasov: Sov. J. Quantum Electron. **21** (1991) 1293.
9) M. A. Franceschini, R. Pini, R. Salimbeni and M. Vannini: Appl. Phys. B **54** (1992) 259.
10) Yu. Bychlov, I. Kostyrya, M. Makarov, A. Suslov and A. Yastremsky: Rev. Sci. Instrum. **65** (1994) 793.
11) R. Marchetti, E. Penco, E. Armandillo and G. Salvetti: J. Appl. Phys. **54** (1983) 5672.
12) R. Gratton, S. Mangioni, J. Niedbalski and R. Valent: J. Phys. E **21** (1988) 851.
13) R. Gratton, S. Mangioni, J. Niedbalski and R. Valent: Rev. Sci. Instrum. **57** (1986) 2634.
14) V. N. Rai and Mayank Shukla: Meas. Sci. Technol. **5** (1994) 1396.
15) E. Nasser: *Fundamentals of Gaseous Ionization and Plasma Electronics* (Wiley-Interscience, New York, 1971) Chap. 3.
16) V. V. Kremnev and Yu. A. Kurbatov: Sov. Phys. Tech. Phys. **17** (1972) 626.
17) H. A. Kramers: Phil. Mag. **46** (1923) 863.